Biosynthesis of bimetallic Au-Ag nanoparticles using Ocimum basilicum (L.) with antidiabetic and antimicrobial properties

Article · January 2015

DOI: 10.5185/amlett.2015.5997

CITATIONS
6

READS
103

4 authors:

Veshara Malapermal
Durban University of Technology
3 PUBLICATIONS **13** CITATIONS
SEE PROFILE

Nonhlanhla Mbatha
University of KwaZulu-Natal
6 PUBLICATIONS **14** CITATIONS
SEE PROFILE

Robert Gengan
Durban University of Technology
47 PUBLICATIONS **319** CITATIONS
SEE PROFILE

K. Anand
University of KwaZulu-Natal
25 PUBLICATIONS **278** CITATIONS
SEE PROFILE

www.amlett.com, www.vbripress.com/aml, DOI: 10.5185/amlett.2015.5997 Published online by the VBRI Press in 2015

Biosynthesis of bimetallic Au-Ag nanoparticles using *Ocimum basilicum* (L.) with antidiabetic and antimicrobial properties

V. Malapermal[1], J.N. Mbatha[1], R.M. Gengan[2], K. Anand[2*]

[1]*Department of Biomedical and Clinical Technology, Faculty of Health Science, Durban University of Technology, Durban, 4001, South Africa*

[2]*Department of Chemistry, Faculty of Applied Science, Durban University of Technology, Durban, 4001, South Africa*

[*]Corresponding author. Tel: (+27) 31 373 5313; E-mail: organicanand@gmail.com

Received: 12 July 2015, Revised: 20 October 2015 and Accepted: 29 October 2015

ABSTRACT

This study was aimed at developing a simple, eco-friendly and cost effective green chemistry method for the synthesis of bimetallic Au-Ag nanoparticles using *Ocimum basilicum* aqueous leaf and flower extracts, respectively as the natural reducing agents. The successive reduction of chloroauric acid and silver nitrate led to the formation of Au-Ag nanoparticles within 10 min at room temperature, suggesting a higher reaction rate than chemical methods involved in the synthesis. Stable, spherical nanoparticles with well-defined dimensions of average size of 3-25 nm was confirmed by UV-Visible spectroscopy, TEM, SEM-EDX, DLS, and zeta potential, whilst, FTIR in combination with GC-MS analyzed the functional groups adhered to the surface of the nanoparticles. The colloidal suspension displayed enhanced antihyperglycemic activity at 69.97 ± 3.42% (leaf) against α-amylase (from porcine) and at 85.77 ± 5.82% (flower) against *Bacillus stearothermophilus* α-glucosidase than that of acarbose and their respective crude extracts. Furthermore, revealed good antibacterial activity against bacterial species *Staphylococcus aureus, Escherichia coli, Bacillus subtilis* and *Pseudomonas aeruginosa.*

Keywords: Ocimum basilicum; bimetallic (Au-Ag) NPs; α-amylase; α-glucosidase; diabetes mellitus.

Introduction

Current worldwide awareness confronts the harsh effects of global warming, climatic change and an alarming rise in the number of debilitating diseases, such as ebola, human immunodeficiency virus infection and acquired immune deficiency syndrome (HIV/AIDS), tuberculosis (TB), diabetes mellitus (DM) and cancer. Therefore, necessitates global change, specifically focusing on minimizing toxicity, using renewable non-depleting materials, avoid hazardous solvents to reduce waste, and the use of safe ingredients that are energy efficient and eco-friendly to the environment.

Many countries undergoing socioeconomic transitions are in the midst of a diabetes epidemic. The global prevalence was estimated at 2.8% in 2000 (171 million people) **[1]**, 382 million people in 2013 and estimated to reach 55% (592 million people) by 2035 if no concerted effort is done to eliminate the progression **[2]**. The reasons for this include changes in lifestyle associated with urbanization, modernization **[3]**, growth of aged population, increasing trends towards obesity, unhealthy diet, sedentary lifestyles **[4]**, with hypertension, coronary heart disease, stroke, genetics and various forms of cancer among the factors contributing to the estimated rise **[5, 6]**. The main challenge in treating DM is that it is no longer treated as a single disorder, but as a collection of conditions with a common result of hyperglycemia and resultant wide-spread multi-organ complications, that may occur in either two common forms, Type I (insulin-dependent diabetes mellitus; IDDM) and Type II (non-insulin-dependent diabetes mellitus; NIDDM) **[7]**. Even though novel antidiabetic agents exists, no major leads have been introduced to find proper drugs for the overall management of DM **[8]**. The current mainstay of oral antidiabetic drugs fails to alter the course of diabetic complications, such as, retinopathy, neuropathy, nephropathy, foot infections and atherosclerosis **[9]**, do not restore glucose homeostasis, pose risks of high secondary failure rates **[10-12]**, increase cardiovascular risk and weight gain **[11]**. Furthermore, drug compliance and accurate regulation of blood glucose is a difficult control process **[13]**. Despite the existence of insulin, that is favoured, it poses many limitations, for example, iatrogenic hypoglycemia, diabetic ketoacidosis, local tissue necrosis, infection, nerve damage, high cost, complex to use and prescribe, potential dosing errors and fear of painful injections that often results in poor patient compliance **[14, 15]**. The disadvantages of synthetic agents

far exceed the advantages, which is an unfortunate outcome that results in many ignorant diabetic patients. Therefore, making the development of effective antidiabetic agents designed to achieve maximal therapeutic efficacy with minimal to no side effects one of the world's top public health priorities. Individuals with diabetes and other fatal debilitating diseases have been treated orally in traditional folk medicine with a variety of plant extracts for many years **[16]**. Natural medicinal drugs are reclaiming their position as the primary source of treatment opposed to the current and main forms of synthetic treatment **[11]**.

Ocimum basilicum (Sweet basil; Lamiaceae) is often used as effective medicine worldwide **[17]**. In many countries, this herb is widely used for culinary purposes, spice, flavors, essential oils and therapeutic applications **[18]**. The leaves and flowering parts of *O. basilicum* are commonly used to treat fever, nausea, abdominal cramps, gastroenteritis, migraines, insomnia, depression, gonorrhea, dysentery, chronic diarrhea and exhaustion. External applications include treatment of acne, loss of smell, insect stings, snake bites and skin infections **[19]**. More importantly, have been identified for its profound antilipidemic, anticholesterol, antimicrobial and antidiabetic properties **[20-23]**. Safety, therapeutic effectiveness, economic benefits and availability are important advantages that *O. basilicum* possesses **[24]**. In addition, their bioactive compounds offer numerous additive health benefits **[25]** and provide a natural source of antioxidants capable of neutralizing free radicals and reducing the severity of diabetic micro- and macrovascular complications **[26]**.

In pursuit of innovative eco-friendly healthcare, phyto-nanotechnology is currently an active source of research focusing on the rapid biogenesis of benign Au, Ag, Fe, Pt, Zn, etc. and metal oxide nanoparticles (NPs) using highly acclaimed medicinal plants as the natural reducing agent **[27]**. Nanotechnology allows scientists to explore, construct and manipulate materials for enhanced specificity, stability, drug encapsulation, biocompatibility and size-dependant characteristics (1-100 nm) **[28]**. Such materials can have profound chemical, physical and biological properties that differ from those of their larger counterparts **[29]**. The success rate of bionanotechnology can be observed in the production of a wide range of products, including foods, cosmetics, drugs, devices, veterinary and tobacco products some of which may use nanotechnology or contain nanomaterials **[30]**. Moreover, provide treatment for various forms of cancer, HIV-1 virus **[31, 32]**, plasmodial **[33]**, fungal or bacterial infections **[34]**, and with current focus directed at its potential antidiabetic effects **[35, 36]**. The future of nanotechnology is to enhance sustainability, this includes developing and using green nanoproducts. To support sustainability, this is the first attempt of introducing the antihyperglycemic and antibacterial assessment of bimetallic Au-Ag nanoparticles (BNPs) formed from *O. basilicum* leaf and flower extracts.

Experimental

Material

Fresh leaves and flowering parts of *O. basilicum* were collected from the Tropical Garden Nursery in KwaZulu Natal (KZN), South Africa (SA). The plants were botanically identified at the KZN Herbarium Durban, SA by Mr M.A. Ngwenya and submitted at the KZN Herbarium where voucher specimens were deposited (voucher: *O. basilicum* L., Det: Malapermal, V., NH0137401) and the solvents absolute ethanol was obtained from Merck (SA) and was of analytical grade. Silver nitrate ($AgNO_3$, ACS reagent) and Gold (III) chloride trihydrate ($HAuCl_4 \cdot 3H_2O$, ACS reagent), type Vi-B from porcine α-amylase; *Bacillus stearothermophilus* α-glucosidase; potato starch; p-nitrophenyl-α-D-glucopyranoside (pNPG); 3,5-dinitrosalicylic acid and sodium potassium tartrate were purchased from Sigma-Aldrich Chemicals (SA) and Acarbose, Glucobay® 50 was obtained from a local pharmacy. Vancomycin 30 µg discs and Gentamycin 10 µg discs were purchased from Davies Diagnostics (SA).

Preparation of crude extracts

O. basilicum crude extracts were prepared by using 10 g each of leaves and flowers that were cleaned, weighed and crushed in a glass beaker. To the respective plant parts 100 ml of 60% EtOH, 70% EtOH and distilled water, respectively were added and left to stand for 24 h. The extract was filtered into a conical flask using a mutton cloth and Whatman No. 1 filter paper. The resultant extract had a 10% concentration and was used as a stock solution **[37, 38]**. The solvents were allowed to evaporate using a rotary evaporator (Heidolph Rotavac) at temperature 40-50°C until a semi solid sticky mass was obtained. The extract was finally freeze dried using a freeze-dryer (Virtis).

Biosynthesis of alloy Au-Ag BNPs

The plant leaf and flower extract were prepared by taking 10 g of thoroughly washed and finely cut leaves and flowers in an Erlenmeyer flask with 100 ml of deionised water, the mixture was boiled for 10 min, and then cooled. Briefly, 10 ml of the plant extract was added drop wise to 30 ml of 1 mM silver nitrate ($AgNO_3$) and vigorously stirred with the aid of magnetic stirrer, until the first color change (brown solution) that indicated the reduction of Ag^+ ions after a few minutes. Then, 30 ml of 2 mM chloroauric acid solution was added in small aliquots of 5 ml at various timed intervals. The reduction of Au^{3+} was revealed after 10 min as shown by stable light violet color of the solution at room temperature. The formation of Au-Ag BNPs was monitored for 36 h.

Characterization techniques

The Au-Ag BNPs were characterized using UV-Vis spectrophotometer (Varian Cary-50 UV spectrophotometer, USA) linked to a TCC-240A Shimadzu heating vessel temperature controlled cell holder in the range of 300-700 nm. The particle size and shape were obtained by conducting TEM analysis, by placing 1 µl of the samples were placed on formvar coated grids, air dried and viewed at 100 kV (JEOL 1010 TEM using a Megaview III camera and iTEM software). For the particles' images and elemental analysis, the samples were prepared by fixing the powder particles to microscope holder, using conducting carbon tape; in addition, subjected to Carl Zeiss, model

EVO HD 15 scanning electron microscope, Germany with EDX detector, Oxford Instruments, UK. FTIR spectra were recorded for the green aqueous leaf and flower extract and BNPs with Bruker Alpha FTIR spectrophotometer. Differential Light Scattering *Malvern Zetasizer Nano ZS* (*Malvern* Instruments Ltd., UK) Merck 2423 instrument was used to measure particle size and zeta potential.

Antibacterial test

The Mueller Hinton agar were seeded with appropriate well mixed overnight nutrient broth culture of each microorganism to 0.5 McFarland turbidity standard: *S. aureus* (ATCC 25923), *E. coli* (ATCC 26922), *P. aeruginosa* (ATCC 27853) and *B. subtilis* (ATCC 6051) at $1x10^6$ colony forming units (CFU) per milliliter. The test organism were streaked evenly on to the surface of the medium with a sterile cotton swab to allow for even growth and wells were cut from the agar plates using a sterile bore **[38]**. The wells were loaded with 30 µl for each sample using a sterile micropipette allowing a 10 min diffusion time. Gentamycin 10 µg, Vancomycin 30 µg discs and 1 mM $AgNO_3$ was used as the positive controls and distilled water used as the negative control. The plates were incubated at 37 ± 2°C for 24 h. The plates were examined for any clearing zones around the walls and/or discs. The zones of inhibition were measured in mm and compared to the controls. This experiment was carried out six times for confirmation and statistical analysis.

Antidiabetic screening

α-Amylase inhibitory test

The effect of time and dose on the inhibitory activity of α-amylase (Type Vi-B from porcine pancreas) were investigated **[39, 40]**.

Time-dependent method: Briefly, 120 µl of the test sample (2 mg/ml for the BNPs suspension and 2 mg/ml for crude extracts), 480 µl of distilled water and 1200 µl of the potato starch (0.5% w/v primed in 20 mM phosphate buffer) were mixed, 600 µl α-amylase (0.05 g of α-amylase prepared in 100 ml ice-cold distilled water) was added to the reaction mixture and incubated at 25 ± 2°C for 3 min. After every 1 min, 200 µl was removed from the reaction mixture and 100 µl of color reagent (96 mM 3,5-dinitrosalicylic acid, 12 g sodium potassium tartrate in 8 ml of 2 M NaOH) was added. The reaction mixture was heated for 15 min at 85 ± 2ºC. After cooling, 900 µl of distilled water was added to the mixture and mixed thoroughly. The optical density (OD) was recorded at 540 nm against the blank. The blank contained 600 µl of distilled water instead of enzyme solution and for the control, test samples were replaced with 120 µl of distilled water and thus represented maximum enzymatic activity. For t = 0 min, a separate experiment was performed, by adding the samples to the DNS solution immediately after addition of enzyme solution. The assay was performed in triplicate. For calculating the percentage inhibition, the following equations were used. Firstly, the net absorbance (A) using equation (1) due to maltose generated was calculated. Secondly, from the net absorbance obtained, the percentage (w/v) of maltose generated was calculated from the equation (2) obtained from the equation in the maltose standard calibration curve (0-2% w/v). Finally, the percentage inhibition was calculated at t = 3 min using equation (3) and 50% inhibition or higher was taken as significant ($p < 0.05$).

OD at 540 nm control or plant extract =
OD_{540nm} Test – OD_{540nm} Blank --------- (1)

% Reaction =
(Mean maltose in sample / Mean maltose in control) × 100
--------- (2)

% Inhibition = 100 - % Reaction --------- (3)

Dose-dependent method: Briefly, 1 ml α-amylase (0.5 unit/ml) primed in 20 mM phosphate buffer (pH 6.9) was pre-incubated for 30 min with a 1 ml test solution (0.0002-2 mg/ml). The reaction was started by the addition of 1 ml potato starch (0.5% w/v, prepared by dissolving in 100 ml distilled water). The reaction mixture was incubated at 25 ± 2ºC for 30 min. Finally, the catalytic reaction was terminated with the addition of 1 ml DNS reagent. The reaction mixture was heated for 15 min at 85 ± 2ºC. The tubes were cooled to room temperature and 9 ml distilled water was added. Individual blanks were prepared for amending the background absorbance; color reagent was added prior to the addition of starch solution and placed in a water bath. For control incubations procedures were the same except that the Au-Ag BNPs suspension was replaced by 1 ml distilled water. The OD was recorded at 540 nm. Antidiabetic medicine acarbose in concentrations of 0.016-1 mg/ml was used as positive control. The assay was performed in triplicate and the mean absorbance was used to calculate percentage of α-amylase inhibition:

$I_{\alpha\text{-Amylase}}\% = (OD_{540nm}\ \text{control} - OD_{540nm}\ \text{sample}/OD_{540nm}\ \text{control}) \times 100$
--------- (4)

α-Glucosidase inhibitory test

The α-glucosidase inhibitory test (Iα-Glucosidase) was performed by preparing, 0.1 ml of 0.5 unit/ml α-glucosidase prepared in ice-cold distilled water that was pre-incubated with 0.1 ml of test samples (range of 0.2 mg/ml and 0.3 mg/ml) for 5 min. Then 0.1 ml of the substrate pNPG 3 mM prepared in 0.01 M phosphate buffer (pH 6.9) was added to start the reaction. After incubation at 37 ± 2ºC for 30 min, the reaction was stopped by adding 1.5 ml of 0.1 M sodium carbonate. Individual blanks were prepared for amending the background absorbance; buffer was added instead of the enzyme. For the control incubations procedures were the same except that the test extract was replaced by buffer. Antidiabetic medicine acarbose in concentrations of 0.00001-1 mg/ml was used as positive control. Enzymatic activity was quantified by measuring the OD at 405 nm. Percentage α-glucosidase activity is calculated by using the following equation (5):

$I_{\alpha\text{-Glucosidase}}\% = (OD_{405nm}\ \text{control} - OD_{405nm}\ \text{sample}/OD_{405nm}\ \text{control}) \times 100$
--------- (5)

IC_{50} values of active Au-Ag BNPs

The potency of Au-Ag BNPs as inhibitors of enzyme catalytic activities of both α-amylase and α-glucosidase was assessed in terms of their IC_{50} values (inhibitor concentration that reduces enzyme activity by 50%) **[41, 42]**. Briefly, aliquots of α-amylase and α-glucosidase enzymes were pre-incubated with increasing concentrations of the Au-Ag suspension and acarbose. Catalytic reactions were started, terminated and enzyme activities determined as above mentioned. The activity of fractions and compounds was assessed by plotting percentage inhibition against a range of concentrations and determining the inhibitory concentration 50% (IC_{50}) value by interpolation of a cubic spline dose-response curve using the GraphPad Prism® 5.03 software.

Inhibition kinetics of α-amylase and α-glucosidase

Modes of inhibition of Au-Ag BNPs on the enzyme activity were determined [**39**]. Briefly, fixed amounts of both α-amylase and α-glucosidase were incubated with increasing concentrations of starch and pNPG, respectively at 37 ± 2ºC for 20 min, in the absence and presence of the Au-Ag suspension (2.5 mg/ml). Reactions were terminated and absorption measurements carried out as above mentioned. The amount of products, reducing sugars as maltose and p-nitrophenol respectively, that are liberated were determined from the corresponding standard curve and then converted to reaction velocities.

Statistical analysis

The statistical analysis of data was expressed as means ± standard error of the mean (SEM). The antibacterial study was analyzed using the Wilcoxon Signed Ranks test and the antidiabetic study were analyzed by one-way and two-way Anova and Bonferroni multiple comparison post test using the GraphPad Prism® 5.03 software.

Results and discussion

UV-Vis studies

A well-defined absorption peak was obtained at 557 nm from the leaf extract (**Fig. 1a**) and 534 nm from the flower extract (**Fig. 1b**), exhibited by the nanometallic Au-Ag particles and consequent color change due to the progressive addition of small aliquots of chloroauric acid solution. The color change from brown to a violet color which rapidly appeared within 10 min confirmed the simultaneous synthesis of two metal nanoparticles. The interaction of nanoparticles with biomolecules of *O. basilicum* leaf and flower extracts, respectively, showed intense peaks therefore, indicating the reduction of Au^{3+} →Au^0 (gold oxidation state) and Ag^+ → Ag^0 (silver oxidation state) thus, *O. basilicum* aq. leaf and flower solution can be used as a natural reducing agent.

TEM analysis

The results obtained from the TEM monograph indicate the size and shape properties of the Au-Ag nanoparticles. Representative TEM images show that the particles were predominantly monodispersed and spherically shaped. As per the method, the rationale for adding Au was to facilitate further stability and for the principle of reducing toxicity of the alloyed BNPs. Previous studies show similar TEM images showing the presence of Au-Ag alloy BNPs **[28, 43]**. The particle size distribution histogram showed a size at 21 ± 11.53 nm of the leaf formed nanoparticles and 25 ± 9.63 nm for the flower formed nanoparticles **(**Supplementary data **[S1])**. These results show it is possible to prepare stable Au-Ag BNPs of size less than 25 nm by varying the ratio of $AgNO_3$, $HAuCl_4$, and the aq. extract of the *O. basilicum* (L.) leaf and flower plant parts.

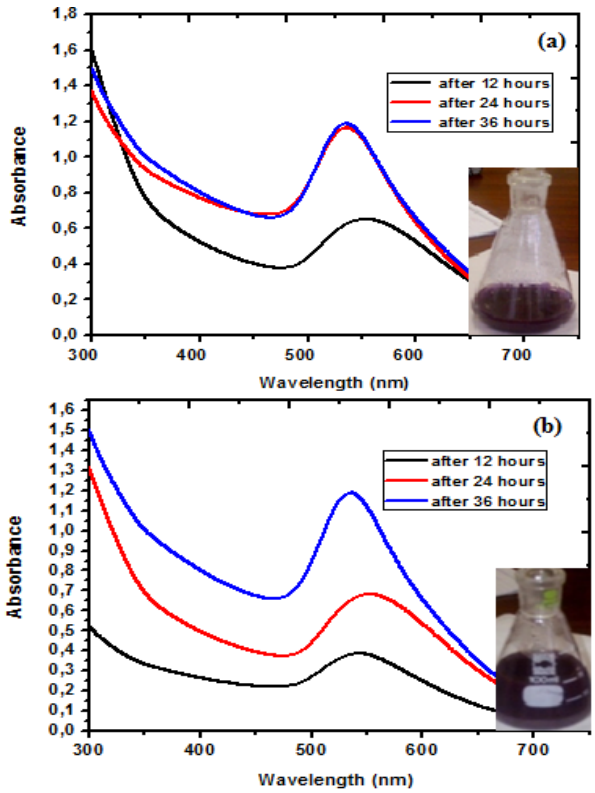

Fig. 1. UV-Visible absorption spectra of BNPs biosynthesized using (a) aq. *O. basilicum* leaf extract and (b) aq. *O. basilicum* flower extracts at different reaction times, both extracts turned a violet color after the addition of 2 mM $HAuCl_4 \cdot 3H_2O$.

SEM-EDX analysis

The crystalline nature of Au-Ag BNPs and nanosize were confirmed by SEM and the EDX pattern. The SEM image showed relatively spherical shape nanoparticles formed with a diameter range of 100 nm. The energy dispersive X-ray analysis revealed signals in silver region and in the gold region at five different areas for both the leaf and flower, respectively, and thus confirmed the formation of Au-Ag BNPs. In addition, an observed spectral signal for oxygen (O) and other element indicated the extracellular organic moieties (originating from *O. basilicum* leaf and flower extracts) were adsorbed on the surface or in the vicinity of the metallic NPs or may originate from the biomolecules that were bound to the surface of the Au-Ag nanoparticles **[S2-S3]**. Peaks for sulfur (S), phosphorus (P) and nitrogen (N) correspond to the protein capping over the BNPs. However, certain elements come from the artifact during sample preparation. Peaks for carbon (C) originate from the grid used.

DLS and zeta potential analysis

DLS analysis showed the size distribution of the particles with an average hydrodynamic size of 73.55 nm and 78.87 nm for the Au-Ag BNPs leaf and flower, respectively, similar to the to the nanoparticles synthesized from the leaf extract of *Melia azedarach* **[30]**. As expected, the particle size obtained from TEM, SEM-EDX and DLS is marginally different due to the varying principles used for measurement. Au-Ag NPs exhibited a stable dispersion of particles evident from the zeta potential of -25.3 mV and -28.4 mV for the Au-Ag NPs synthesized from the leaf and flower, respectively. A zeta potential with higher magnitude potentials (20-40 mV) indicates a stable system **[45] [S4]**. Many reports have proposed that surface active molecules can stabilize the nanoparticles and reaction of the metal ions is possibly facilitated by reducing sugars and or terpenoids **[44]**. Organic molecules such as carotenoids, vitamins, minerals, amino acids, sterols, glycosides, alkaloids, flavonoids, terpenes and phenolics can act as surface active molecules responsible for stability and the Au-Ag BNPs successive formation **[45, 46]**.

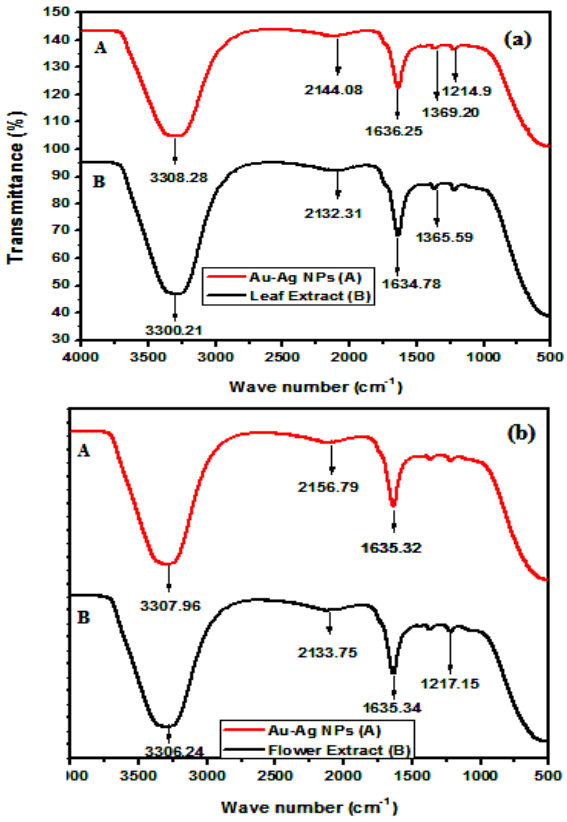

Fig. 2. (a) FTIR spectra (A) FTIR Profile of BNPs biosynthesized using *O. basilicum* leaf extract and (B) aq. *O. basilicum* leaf extract and (b) FTIR spectra (A) FTIR Profile of BNPs biosynthesized using *O. basilicum* flower extract and (B) aq. *O. basilicum* flower extract.

GC-MS analysis

The chemical composition of the leaf and flower aq. and EtOH extract of *O. basilicum* (L.) were determined via GC-MS analysis using Shimadzu GC-2010 Plus with GC-MS-QP2010SE equipped with a split/splitless capillary injection port. The capillary column used was a GL Sciences InertCap 5MS/Sil Length 30mm, I.D. 0.25mm, film thickness 0.25µm. Chemical constituents were identified after comparison with those available in the computer library (NIST) attached to the GC-MS instrument. The main organic compounds that were identified in *O. basilicum* leaf extract include: Cyclohexanol; Menthol; Hexanedioic acid/Adipic acid; 3, 7, 11, 15-Tetramethyl-2-hexadecen-1-ol; 13-Methyl-14-pentadecene-1, 13-diol; and terpenes such as Squalene and Phytol **[Table S1]**. Some of the compounds detected in this study were consistent with those of previously published studies in which chemical components were isolated by various organic solvent extractions **[47]** and concluded that the variation in chemical composition of *O. basilicum* (L.) could depend on the climatic and geographical conditions of the parent plant **[48]** in SA.

FTIR studies

FTIR was used to identify any potential biomolecules, present in the leaf and flower extract, which are responsible for reducing, biocapping and provide efficient stabilization of Ag^{+} and Au^{3+} ions to Ag^{0} and Au^{0}. FTIR spectra (**Fig. 2 (a)** and **(b)**) of the crude aqueous extract and Au-Ag BNPs showed a stretching frequency from 3300.21 to 3308.28cm^{-1} for leaf and 3306.24 to 3307.96cm^{-1} for the flower derived BNPs suggesting an O-H vibration from the phenolic functional group and the possible biocapping of Ag and Au NPs after reducing silver nitrate and chloroauric acid, whereas peaks at 1217cm^{-1} can be attributed to the ether linkages. From the leaf derived Au-Ag BNPs C-H and nitro stretch were obtained. Previous reports indicate the partial role of phenolic hydroxyls in the reduction mechanism by donating electrons and forming quinones that possess a stronger ability to interact with nanoparticles. Therefore, the secondary metabolites containing hydroxyl groups may act as capping agents and further facilitate the formation of stable metal nanoparticles **[49]**. Furthermore a shift from 1634.78 to 1636.25cm^{-1} and 1635.34 to 1635.32cm^{-1} from the leaf and flower derived BNPs, respectively shows a carbonyl (C=O) stretch, which may be assigned to the amide I bond or proteins arising due to the carbonyl stretch, suggesting that proteins are interacting with the biosynthesized nanoparticles and that their secondary structure were not affected during the reaction with Ag^{+} and Au^{3+} ions or after binding with Ag and Au nanoparticles. The chemical compounds identified in the present study together with previous phytochemical reports on *O. basilicum* leaf and flower extracts suggest that polyphenols, carbonyl groups, flavonoids, alkaloids, terpenoids, amines, carbohydrates, pigments **[22, 50]**, and additional reducing biomolecules, secondary metabolites, proteins and lipids present in the plant leaf and flower parts, at different concentrations may be responsible for the bioreduction of Ag^{+} and Au^{3+} ions. Thus, further studies are recommended to unravel the role of the biomolecules derived from *O. basilicum* leaf and flower extracts for a more detailed understanding of the bioreduction phenomena. **Scheme 1** illustrates a proposed reduction mechanism for synthesizing Au-Ag BNPs from phenolic rich plants such as *O. basilicum*. Representing a proton transfer reaction whereby phenolic groups are converted to keto groups and metal salts are converted to zero (0) state metal nanoparticles.

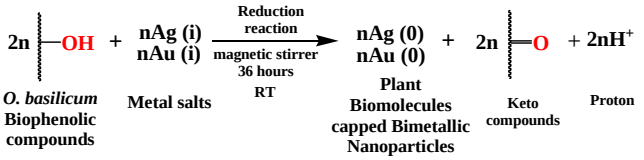

Scheme 1. Proposed mechanism was elucidated using phenolic compounds in the formation of Au-Ag BNPs; *RT = Room Temperature.*

Antibacterial activity

The extracts derived from *O. basilicum* have been much exploited traditionally and commercially for their profound antibacterial and antifungal properties **[22]**. The diverse chemical composition within *O. basilicum* and rich source of phenolic (-OH) constituents suggests that the medicinal properties of plants depend on the specific chemical groups isolated. Compounds with antimicrobial value include phenols, terpenoids, flavonoids, carbohydrates, tannins and quinones **[22,51]**. In the current study, the green synthesis of BNPs capped with these important phytochemicals contributes to the enhanced properties of the phytochemical mixture.

Table 1. Zones of Inhibition in (mm) for Au-Ag BNPs against the various bacterial test strains.

Samples	*B. subtilis* [a]	*E. coli* [a]	*P. aeruginosa* [a]	*S. aureus* [a]	*S. aureus* [b]
BNPs leaf [c]	1.000 ± 0.000	3.333 ± 0.211	5.167 ± 0.167	6.167 ± 0.601	2.333 ± 0.333
BNPs flower [c]	NI	NI	1.667 ± 0.211	3.500 ± 0.719	1.333 ± 0.333
Control (1 mM $AgNO_3$)[c]	2.000 ± 0.000	1.500 ± 0.224	2.000 ± 0.000	2.333 ± 0.422	2.000 ± 0.000
+ Control (Gentamycin 10 µg)	10.000 ± 0.000	5.000 ± 0.000	6.000 ± 0.000	-	-
+ Control (Vancomycin 30 µg)	-	-	-	7.000 ± 0.000	3.000 ± 0.000
OB 10% aq. leaf extracts[c]	NI	NI	NI	NI	NI
OB 10% aq. flower extracts[c]	NI	NI	NI	NI	NI
- Control (Distilled water) [c]	NI	NI	NI	NI	NI

Results are expressed as mean inhibition ± SEM, N = 6; OB= *O. basilicum*; NI = No Inhibition. a. Grouping variable: 100 µl of bacteria per plate, b. Grouping variable: 200 µl of bacteria per plate, c. 30 µl of sample

This is especially significant to overcome antimicrobial resistance with greater beneficial outcomes and at a lower toxicity to humans **[52, 53]**. The highest antibacterial activity was observed against *P. aeruginosa* (5.167 ± 0.167) using BNPs synthesized from *O. basilicum* leaf extract, p-value 0.025, followed by *E. coli* (3.333 ± 0.211), p-value 0.014 compared to Gentamycin **[S5]**. The only and lowest inhibition was observed against *P. aeruginosa* using BNPs synthesized from the flower extract (1.667 ± 0.211), p-value 0.023. The inhibition of the BNPs against *S. aureus* was tested at two grouping variables, at 100 µl and 200 µl bacteria per plate, respectively. The BNPs derived from the leaf extract showed inhibition against *S. aureus* at 100 µl of bacteria per plate (6.167 ± 0.601), p-value 0.238 and inhibition of BNPs (derived from flower extracts) (3.500 ± 0.719), p-value 0.026 compared to Vancomycin (7.000 ± 0.000). The BNPs derived from the leaf extract showed half the inhibition at 200 µl bacteria per plate (**Table 1**). Therefore, coupling the inherent bactericidal properties of *O. basilicum* with that of the synthesized BNPs proved to be beneficial to minimize the dose needed to be administered for total antibacterial reduction against Gram-negative and Gram-positive bacteria, at a low concentration of Ag present with Au. The enhanced antibacterial properties of Au-Ag BNPs may be possible due to the more highly reactive silver atoms in combination with gold, thus inducing an electron transfer reaction that was confirmed by the negative charge in the zeta potential analysis, this led to adherence on the bacterial cell surface causing membrane damage and hence cell death **[54]**.

Inhibitory effects of Au-Ag BNPs on α-Amylase and α-Glucosidase activity

Control of postprandial hyperglycemia (PPHG) is an important strategy and a therapeutic approach to manage diabetes, specifically Type 2 diabetes **[55]**. The enzyme activity of human pancreatic α-amylase (HPA) and α-glucosidase in the small intestine correlates to an increase in postprandial glucose levels. After a mixed carbohydrate diet pancreatic α-amylase catalyzes the initial step in hydrolysis of starch to a mixture of smaller oligosaccharides comprising of maltose, maltotriose, and a number of α-(l-6) and α-(1-4) oligoglucans that are finally converted to monosaccharides by α-glucosidase and further degraded to glucose **[56]**. Liberated glucose is absorbed by the gut, enters the bloodstream and results in a high blood glucose level **[25]**. Therefore, the inhibition of α-amylase activity and inhibition of α-glucosidase **[57]** have been targeted as potential avenues for modulation of PPHG in diabetic patients, through mild inhibition of the enzymatic breakdown of complex carbohydrates to decrease meal-derived glucose absorption **[58]** so that glucose levels in the blood can return to normal limits. The BNPs synthesized from *O. basilicum* leaf extracts demonstrated inhibitory activity (69.67 ± 3.42%, p-value < 0.0001) that was greater than that of acarbose, p-value 0.0002, demonstrated in an uncompetitive manner, this suggests that some of the α-amylase inhibitory components in the BNPs suspension bind only to the enzyme-substrate complex and may distort the active site. BNPs (flower) represented high inhibition 60.57 ± 3.15%, p-value 0.006 compared to acarbose in a non-competitive manner, similar to the mode of inhibition of acarbose which can be mixed non-competitive on α-amylase activity as shown in previous studies **[25].** Both BNPs derived from leaf and flower, respectively appeared to be good inhibitors of α-amylase at a dose as low as 0.0002 mg/ml. All crude *O. basilicum* extracts demonstrated high inhibition than the standard control, acarbose. However, *O. basilicum* flower ethanolic extract and leaf aq. extract, respectively demonstrated the highest inhibitory activity (61.73 ± 6.37%, p-value 0.011 and 61.23 ± 5.24%, p-value 0.007, respectively). The *O. basilicum* leaf ethanolic extract demonstrated the lowest inhibitory activity (55.13 ± 9.17%, p-value 0.027) against α-amylase. The lowest IC_{50} value was obtained with *O. basilicum* leaf extract prepared in EtOH 70% and thus appeared to be

better inhibitors of α-amylase to that of acarbose **[Table S2]**.

Inhibitory activities of the crude extracts and BNPs were tested for their hypoglycaemic activity as a single dose and dose-response against *B. stearothermophilus* α-glucosidase. BNPs (flower) demonstrated the highest percentage inhibition against *B. stearothermophilus* α-glucosidase activity (85.77 ± 5.82%) in an uncompetitive manner, followed by BNPs (leaf) (78.62 ± 12.65%) **[S6]** displaying a mixed type inhibition. Both leaf and flower BNPs appeared to be good inhibitors (low IC_{50}), similar to that of acarbose (**Table 2**). The crude leaf extracts (70% EtOH) demonstrated a percentage inhibition at 69.89 ± 6.87%; followed by leaf 60% EtOH extracts (50.50 ± 3.594%). Both extracts showed good inhibition of α-glucosidase at a dose-response. The aq. leaf extract of *O. basilicum* yielded statistically the lowest inhibitory activity (34.75 ± 3.705%) compared to acarbose, p-value 0.044. The properties of *O. basilicum* and have long been compared in several phytochemical parameters **[59]**.

Table 2. Inhibitory action of Au-Ag BNPs and crude extracts on α-Glucosidase activity

Samples	α-Glucosidase inhibition % [a] 0.3 mg/ml; [b] 0.2 mg/ml	p-value	IC_{50} (mg/ml) [a] 0.0003-0.3 mg/ml [b] 0.0002-0.2mg/ml
Acarbose	73.75 ± 12.86	0.0023	0.001
BNPs leaf [b]	78.62 ± 12.65	0.0249	0.004 [b]
BNPs flower [b]	85.77 ± 5.82	0.0001	0.001 [b]
70% EtOH leaf [a]	69.89 ± 6.871	< 0.0001	0.007 [a]
Aq. dist. leaf [a]	34.75 ± 3.705 *	0.0026	10.55 [a]
60% EtOH leaf [a]	50.50 ± 3.594	0.0008	0.002 [a]

*Results are expressed as mean ± SEM; N = 3; p < 0.05, p-value summary * vs control; Aq. dist. = Aqueous distillation.*

Thus, it is anticipated that certain plant phytochemicals such as phenolics **[58]**, flavonoids and other important bioactive compounds previously highlighted **[20, 53]** were present in the phytochemical mixture with the synthesized Au-Ag BNPs. The significant biological activity displayed by *O. basilicum* derived Au-Ag BNPs compared to their various crude extracts and acarbose may be due to the increasing the surface area phenomenon (promoting electron transfer reaction from adjacent Ag atoms to Au atoms) and increased pharmacokinetics thereafter, thus, contributing to the enhanced inhibition of Gram-positive and Gram-negative bacterial cells, α-amylase and α-glucosidase enzymes. *O. basilicum* crude leaf and flower extracts possess notable inhibitory α-amylase and α-glucosidase potential, whereas the forms of Au-Ag BNPs have proven to possess greater biological activity by varying the doses. The simple, rapid, non-toxic, eco-friendly green synthesis method generated Au-Ag BNPs, with varied size, composition, and structure that can offer the potential to tune the biological/catalytic activity on the BNPs surface structure for improved applications in catalytic reduction, biosensor devices, debromination, dechlorination, electrochemistry, and remediation **[43]**. In comparison to monometallic nanoparticles, Au-Ag BNPs creates a synergistic effect between the two metals, thus displayed greater catalytic properties that can be used in lowering hyperglycemia through inhibition of diabetic related carbohydrate metabolizing enzymes. Furthermore, BNPs can target Gram-negative and Gram-positive bacteria, and simultaneously prevent long-term diabetic complications such as peripheral neuropathy that predisposes bacterial infections. This phytochemical mixture can be included in diet to cure associated diabetic induced infections as well as to inhibit hydrolysis of starch into di- and monosaccharaides giving dual relief to diabetic patients. Henceforth, further *in vivo* pharmacokinetic and toxicity studies are encouraged. With little uncovered mechanism in the current study, there is a wide scope for detailed investigation for more effective application of Au-Ag BNPs in diabetes therapy. In addition, the exact mode of the binding of nanoscale molecules to α-amylase and α-glucosidase and consequent inhibition of the enzyme is another interesting point that merits further investigation.

Conclusion

In conclusion, an environmentally benign and facile phytochemical route synthesized bimetallic Au-Ag nanoparticles at room temperature. This method used green catalysis as opposed to harsh chemical reducing agents (e.g., $NaBH_4$, sodium citrate) and physical techniques. This bio-derived metallic nanoparticle showed excellent enhanced inhibitory enzymatic/antibacterial properties. The quality of phytochemicals absorbed from *O. basilicum* extract can be efficiently used in the synthesis of BNPs via a green chemistry route. The nanoparticles formation was characterized by spectroscopic techniques (UV-Vis spectra) and the size, morphology and elemental analysis were confirmed by TEM and SEM-EDX. The stability of the nanoparticles was confirmed by zeta potential. Finally, the FTIR in correlation with GC-MS identified the biomolecules responsible for bioreduction and capping of the nanoparticles.

Acknowledgements

Sincere gratitude to Ms. T.S. Ndolvu (Microbiology, Durban University of Technology), Mr. C. Phillip (Electron Microscope Unit, University of KwaZulu Natal) for TEM measurements, Mr. M.A. Ngwenya from the KwaZulu Natal Herbarium for identifying the plant species and thanks to the Durban University of Technology - South Africa for funding this project.

Reference

1. Wild, S.; Roglic, G.; Green, A.; Sicree, R.; King, H. *Diabetes care* **2004**, *27*, 1047. **DOI:** 0.2337/diacare.27.5.1047
2. Guariguata, L.; Whiting, D. R.; Hambleton, I.; Beagley, J.; Linnenkamp, U.; Shaw, J. E.; *Diabetes Res. Clin. Pract.* **2014**, *103*, 137. **DOI:** 10.1016/j.diabres.2013.11.002
3. Hamdan, I. I. and Afifi, F. U. J. *Ethnopharmacol.* **2004**, *93*, 117. **DOI:** 10.1016/j.jep.2004.03.033
4. Hannan, J. M.; Marenah, L.; Ali, L.; Rokeya, B.; Flatt, P. R.; Abdel-Wahab, Y. H. *J. Endocrinol.* **2006**, *189*, 127. **DOI:** 10.1677/joe.1.06615
5. Omran, A. J. *Trop. Pediatr.* **1983**, *29*, 305. **DOI:** 10.1093/tropej/29.6.305
6. Reddy, P.; Steyn, K.; Saloojee, Y. *Circulation* **1998**, *97*, 596. **DOI:** 10.1161/01.CIR.97.6.596
7. Nguyen, T. H.; Um, B. H.; Kim, S. M. *J. Food Sci.* **2011**, *76*, 208. **DOI:** 10.1111/j.1750-3841.2011.02391
8. Bastaki, S. *Int. J. Diabetes Metab.* **2005**, *13*, 111. **DOI:** 10.4172/2155-6156.1000587
9. Reid, M. J. A.; Tsima, B. M.; Kirk, B. *Afri. J. Diabetes Med.* **2012**, *20*, 28. **DOI:**10.3366/E0001972008000405

10. Premila, M. S.; Conboy, L. *J. Altern. Complementary Med.* **2006**, *13*, 841. **DOI:** 10.1089/acm.2007.0608
11. Avery, M. A.; Mizuno, C. S.; Chittiboyina, A. G.; Kurtz, T. W.; Pershadsingh, H. A. *Curr. Med. Chem.* **2008**, *15*, 61. **DOI:** 10.2174/092986708783330656
12. Chiha, M.; Njeim, M.; Chedrawy, E. G. *Int. J. Hypertens.* **2012**, 7. **DOI:** 10.1155/2012/697240
13. Rang, H. P.; Dale, M. M.; Ritter, J. M.; Moore, P. K. Pharmacology; Churchill Livingstone: Scotland, **2003**.
14. Mo, R.; Jiang, T.; Di, J.; Tai, W.; Gu, Z. *Chem. Soc Rev.* **2014**, *43*, 3595. **DOI:** 10.1039/c3cs60436e
15. Cryer, P. E. *Endocr. Pract.* **2008**, *14*, 750. **DOI**: 10.2337/db14-0059
16. Ezuruike, U. F.; Prieto, J. M. *J. Ethnopharmacol.* **2014**, *155*, 857. **DOI:** 10.1016/j.jep.2014.05.055
17. Tchoumbougnang, F.; Zollo, P. H. A.; Avlessi, F.; Alitonou, G. A.; Sohounhloue, D. K.; Ouamba, J. M.; Tsomambet, A.; Okemy-Andissa, N.; Dagne, E.; Agnaniet, H.; Bessiere, J. M.; Menut, C. J. *Essent. Oil Res.* **2006**, *18*, 194. **DOI:** 10.1080/10412905.2006.9699064
18. Bilal, A.; Jahan, N.; Ahmed, A.; Bilal, S. N.; Habib, S.; Hajra, S. I. *J. Curr. Res. Rev.* **2012**, *4*, 73. **DOI :** 10.15373/22778179
19. Kaya, I.; Yiğit, N.; Benli, M. *Afr. J. Tradit., Complementary Altern. Med.* **2009**, *5*, 363. **DOI:** 10.1007/s10072-014-1913-3
20. Benalla, W.; Bellahcen, S.; Bnouham, M. *Curr. Diabetes Rev.* **2010**, *6*, 247. **DOI:** 10.2174/157339910791658826
21. Jaiganesh, K. P.; Baskar, N.; Ramasamy, N.; Arunachalam, G. J. *Sci. Res. Pharm.* **2012**, *1*, 102. **DOI:** 10.1248/cpb.37.1279
22. Usman, L. A.; Ismaeel, R. O.; Zubair, M. F.; Saliu, B. K.; Olawore, N. O.; Elelu, N. *Int. J. Chem. Biochem. Sci.* **2013**, *3*, 47.
23. Zeggwagh, N. and Eddouks, M. *Am. J. Pharmacol. Toxicol.* **2007**, *2*, 123. **DOI:** 10.3844/ajptsp.2007.123.129
24. Dineshkumar, B.; Mitra, A.; Manjunatha, M. *Int. J. Green Pharm.* **2010**, *4*, 115. **DOI:** 10.4103/0973-8258.63887
25. Nickavar, B. and Yousefian, N. *Iran. J. Pharm. Res.* **2009**, *8*, 53. **DOI:** 10.1016/j.cis.2012.12.001
26. Swarnalatha, L.; Rachela, C.; Ranjanb, S.; Baradwaj, P. *Int, J. Nanomater. Biostruct.* **2012**, *2*, 25. **DOI:** 10.1186/2228-5326-2-9
27. Madhumitha, G. and Roopan S.M. *J. Nanomater.* **2013**, *2013*,1. **DOI:** 10.1155/2013/951858
28. Meena Kumari, M.; Jacob, J.; Philip, D. *Spectrochim. Acta, Part A Biomol. Spectrosc.* **2015**, *137*, 185. **DOI:** 10.1016/j.saa.2014.08.079
29. Mubarak, A. D.; Thajuddin, N.; Jeganathan, K.; Gunasekaran, M. *Colloids Surf., B.* **2011**, *85*, 360. **DOI:** 10.1016/j.colsurfb.2011.03.009
30. Sukirtha, R.; Priyanka, K. M.; Antony, J. J.; Kamalakkannan, S.; Ramar, T.; Palani, G.; Krishnan, M.; Achiraman, S. *Process Biochem.* **2012**, *47*, 273. **DOI:** 10.1016/j.procbio.2011.11.003
31. Gavanji, S.; Mohabatkar, H.; Baghshahi, H.; Zarrabi, A. I. J. *Scientific Res. in Knowledge* **2014**, *2*, 67. **DOI:** 10.12983/ijsrk-2014-p0067-0074
32. Ehdaie, B. *Int. J. Biol. Sci.* **2007**, *3*, 108. **DOI:** 10.7150/ijbs.3.108
33. Panneerselvam, C.; Murugan, K.; Amerasan, D. *Adv. Mater. Res.* **2015**, *1086*, 11. **DOI:** 10.4028/www.scientific.net/AMR.1086.11
34. Rout , Y.; Behera, S.; Ojha, A. K.; Nayak, P. L. *J. Microbiol. Antimicrob.* **2012**, *4*, 103. **DOI:** 10.5897/JMA11.060
35. Woldu, M. A. and Lenjisa, J. L. *Int. J. Basic Clin. Pharmacol.* **2014**, 3, 277. **DOI:** 10.5455/2319-2003.ijbcp20140405
36. Alkaladi, A.; Abdelazim, A.M.; Afifi, M. *Int. J. Mol. Sci.* **2014**, *15*, 2015. **DOI:** 10.3390/ijms15022015
37. Ahmad, I. and Beg, A. Z. *J. Ethnopharmacol.* **2001**, *74*, 113. **DOI:** 10.1016/s0378-8741(00)00335-4
38. Sivaranjani, K. and Meenakshisundaram, M. *Int. Res. J. Pharm.* **2013**, *4*, 225. **DOI:** 10.7897/IRJP/2230-8407 on page 786
39. Ali, H.; Houghton, P. J.; Soumyanath, A. *J. Ethnopharmacol.* **2006**, *107*, 449. **DOI:** 10.1016/j.jep.2006.04.004
40. Aujla, M. I.; Ahmed, D.; Khair-ul-Bariyah, S. *Pak. J. Chem.* **2012**, *2*, 134. **DOI:** 10.15228/2012.v02.i03.p06
41. Mogale, M. A.; Lebelo, S. L.; Thovhogi, N.; de Freitas, A. N.; Shai, L. J. *Afr. J. Biotechnol.* **2009**, *10*, 15033. **DOI:** 10.5897/AJB11.1408
42. Cheng, Y. and Prusoff, W. H. *Biochem. Pharmacol.* **1973**, *22*, 3099. **DOI:** 10.1093/nar/gkp253
43. Sheny, D. S.; Mathew, J.; Philip, D. *Spectrochim. Acta, Part A Biomol. Spectrosc.* **2011**, *79*, 254. **DOI:** 10.1016/j.saa.2011.02.051
44. Song, J. Y. and Kim, B. S. *Bioprocess Biosyst. Eng.* **2009**, *32*, 79. **DOI:** 10.1007/s00449-008-0224-6
45. Gengan, R. M.; Anand, K.; Phulukdaree, A.; Chuturgoon A. *Colloids Surf., B.* **2013**, *105*, 87. **DOI:** 10.1016/j.colsurfb.2012.12.044
46. Huang, J.; Li, Q.; Sun, D.; Lu, Y.; Su, Y.; Yang, X.; Wang, H.; Wang, Y.; Shao, W.; Ning, H.; Hong, J.; Chen, C. *Nanotechnology* **2007**, *18*, 104. **DOI:** 10.1088/0957-4484/18/10/105104
47. Lee, S. J.; Umano, K.; Shibamoto, T.; Lee, K. G. *Food Chem.* **2005**, *91*, 131. **DOI:** 10.1016/j.foodchem.2004.05.056
48. Saha, S.; Dhar, T. N.; Sengupta, C.; Ghosh, P. *Czech J. Food Sci.* **2013**, *31*, 194.
49. Yallappa, S.; Manjanna, J.; Dhananjaya, B. J. *Spectrochim. Acta, Part A Biomol. Spectrosc.* **2015**, *137*, 236. **DOI:** 10.1016/j.saa.2014.08.030
50. Roopan, S. M.; Surendra, T. V.; Elango, G.; Kumar, S. H. *Appl. Microbiol. Biotechnol.* **2014**, *98*, 5289. **DOI:** 10.1007/s00253-014-5736-1
51. Hussain, A. I.; Anwar, F.; Hussain Sherazi, S. T.; Przybylski, R. *Food Chem.* **2008**, *108*, 986. **DOI:** 10.1016/j.foodchem.2007.12.010
52. Swartjes, J. J.; Sharma, P. K.; van Kooten, T. G.; van der Mei, H. C.; Mahmoudi, M.; Busscher, H. J.; Rochford, E. T. *Curr. Med. Chem*. **2014**. **DOI:** 10.2174/09298673216661409161213 55
53. Lokina, S.; Stephen, A.; Kaviyarasan, V.; Arulvasu, C.; Narayanan, V. *Eur. J. Med. Chem.* **2014**, *76*, 256. **DOI:** 10.1016/j.ejmech.2014.02.010
54. Banerjee, M.; Sharma, S.; Chattopadhyay, A.; Ghosh, S. S. *Nanoscale* **2011**, *3*, 5120. **DOI:** 10.1039/C1NR10703H
55. Elya, B.; Basah, K.; Mun'im, A.; Yuliastuti, W.; Bangun, A.; Septiana, E. K. *J. Biomed. Biotechnol.* **2012**, *2012*, 281078. **DOI:** 10.1155/2012/281078
56. Sudha, P.; Zinjarde, S.; Bhargava, S.; Kumar, A. *BMC Complementary Altern. Med.* **2011**, *11*, 5. **DOI:** 10.1186/1472-6882-11-5
57. Subramanian, R.; Asmawi, M. Z.; Sadikun, A. *Acta Biochim. Pol.* **2008**, *55*, 391. **DOI:** 10.1186/1472-6882-13-39
58. McCue, P. P. and Shetty, K. *Asia Pac. J. Clin. Nutr.* **2004**, *13*, 101. **DOI:**10.1016/j.jscs.2011.04.006
59. Dev, N.; Das, A. K.; Hossain, M. A.; Rahman, S. M. M. *J. Sci. Res.* **2011**, *3*, 197. **DOI:** 10.3329/jsr.v3i1.5409

Supporting information

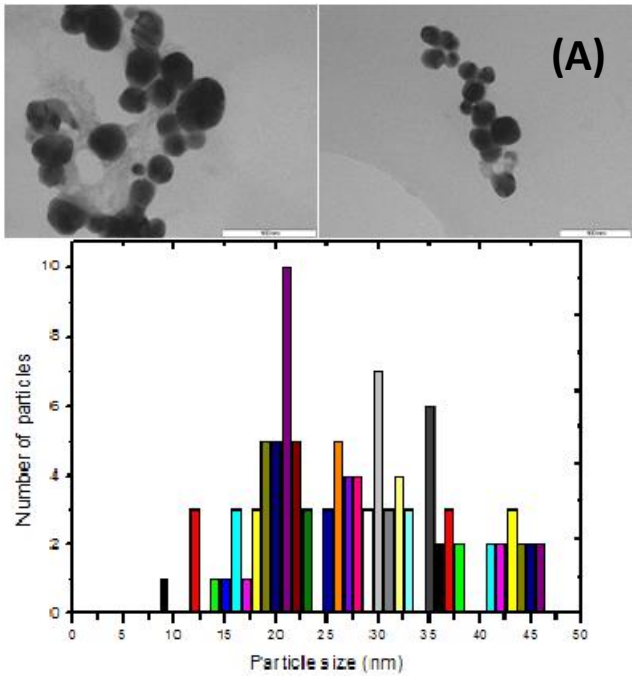

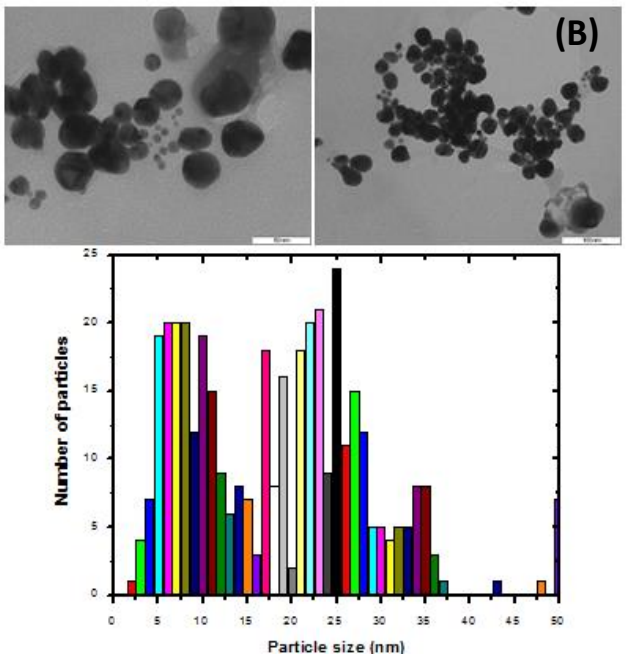

Fig. S1. (A) Representative TEM micrograph of Au-Ag BNP biosynthesized by aq. leaf extracts of *O. basilicum* and histogram representation of size distribution of Au-Ag BNP (std. dev. 21 ± 11.53) and (B) Representative TEM micrograph of Au-Ag BNP biosynthesized by aq. flower extracts of *O. basilicum* and histogram representation of size distribution of Au-Ag BNP (std. dev. 25 ± 9.63).

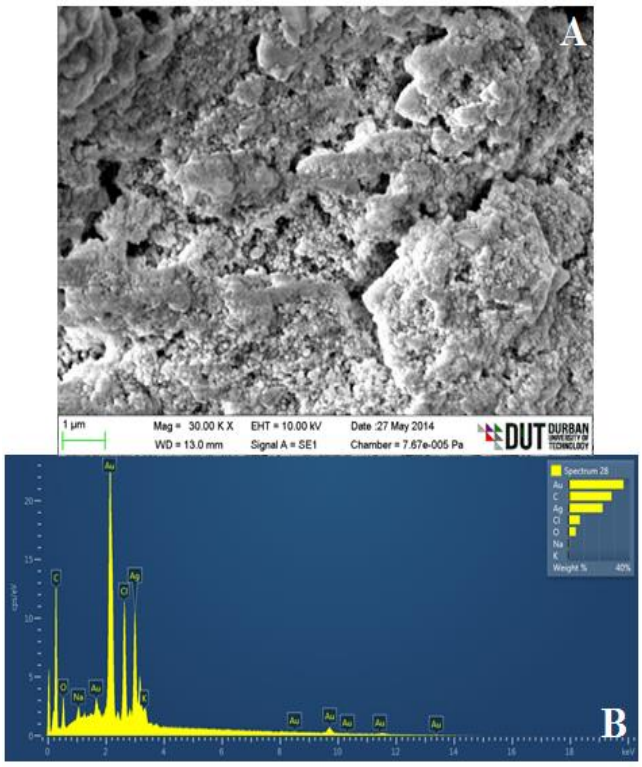

Fig. S2. (A) SEM with EDX image of Ag-Au BNPs biosynthesized by aq. leaf extracts of *O. basilicum* and EDX showed the presence of the elements on the surface of the Au-Ag BNP**.**

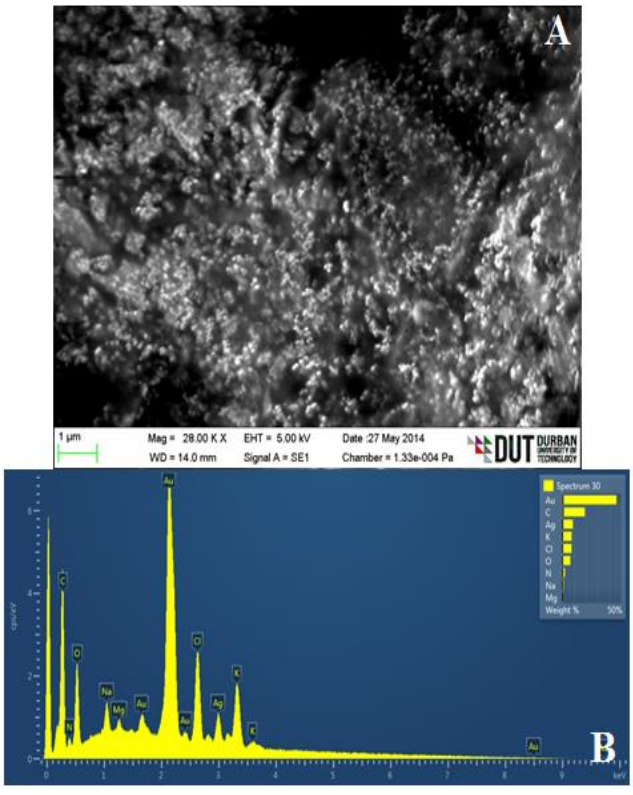

Fig. S3. (A) SEM with EDX image of Ag-Au BNPs biosynthesized by aq. flower extracts of *O. basilicum* and EDX showed the presence of the elements on the surface of the Au-Ag BNP.

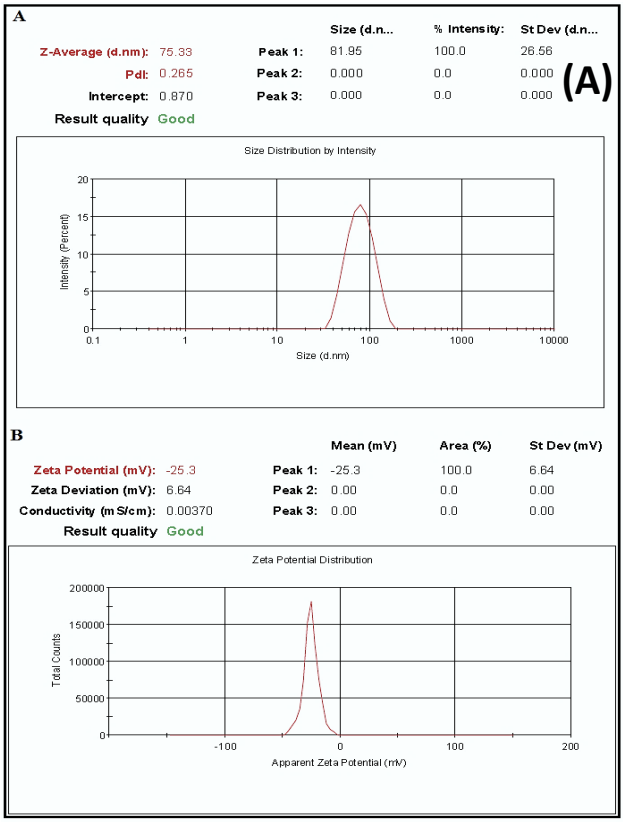

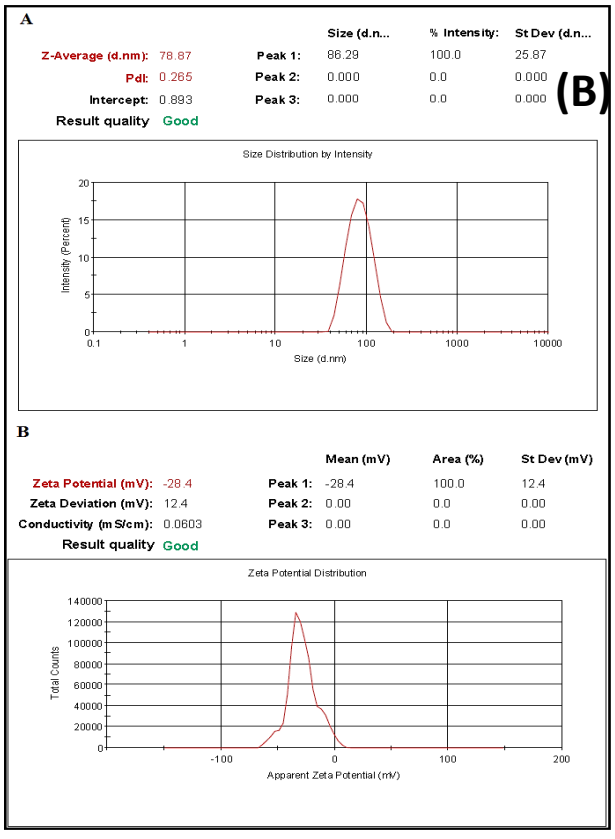

Fig. S4. DLS profile (A) Size distribution of *O. basilicum* leaf Au-Ag BNPs with maximum intensity at 73.55 nm and stability at -25.3 mV in zeta potential analysis (B) Size distribution of *O. basilicum* flower Au-Ag BNPs maximum intensity at 78.87 nm and stability at -28.4 mV in zeta potential analysis.

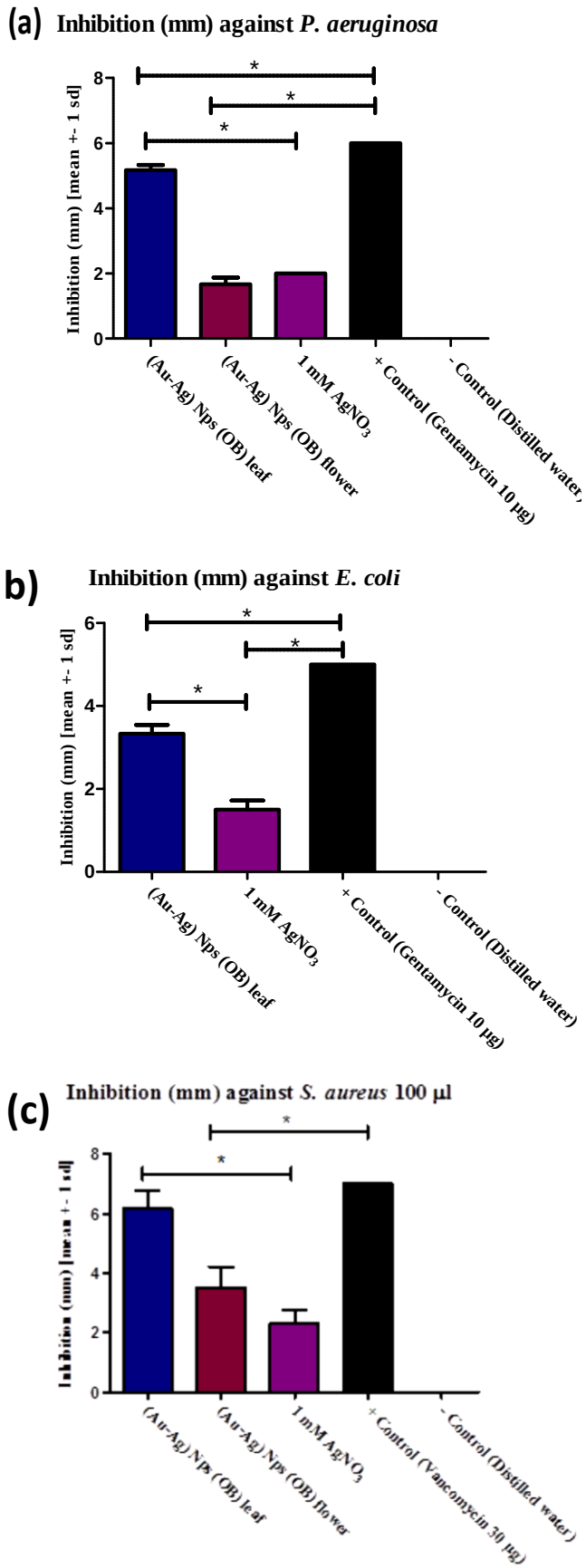

Fig. S5. Mean inhibition (mm) against (a) *P. aeruginosa*, (b) *E. coli*, and (c) *S. aureus* at 100 µl/plate. *The mean inhibition (mm) ± SEM, N = 6, and comparisons of BNPs against all control groups. All values p < 0.05, p-value summary * show a significant difference in the central (median) value; OB = O. basilicum.*

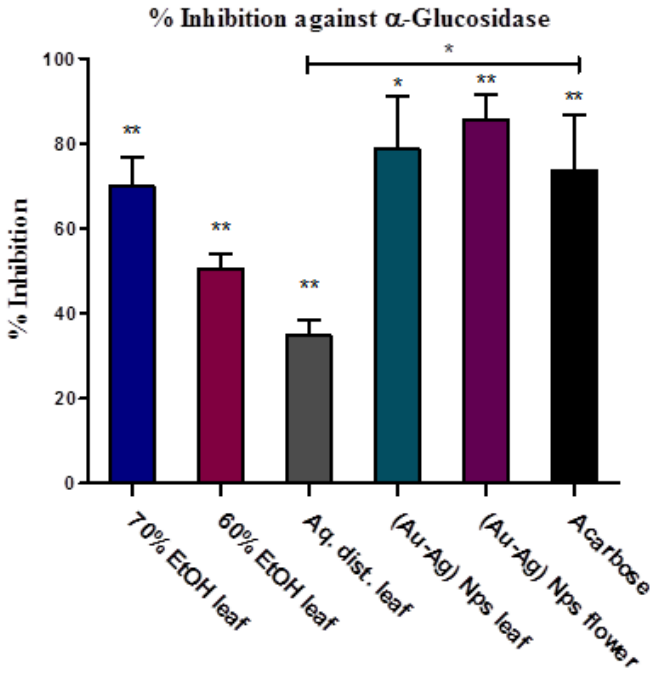

Fig. S6. Inhibitory activities of various crude *O. basilicum* leaf extracts (0.3 mg/ml), and BNPs biosynthesized from *O. basilicum* leaf and flower, respectively at concentration 0.2 mg/ml and 1 mg/ml for acarbose, tested for their hypoglycaemic activity using α-glucosidase as a model.
*Results expressed as % mean ± SEM, N = 6; p < 0.05, p-value summary * and p < 0.01, p-value summary **; Aq. dist. = Aqueous distillation*

Table S1. GC-MS results indicating the chemical constituents identified in *O. basilicum* (A) EtOH and (B) aqueous leaf extract.

(A)

Peak no.	Compound	MF	MW (g/mol)	RT (min)	Area (%)
1	3,7,11,15-Tetramethyl-2-hexadecen-1-ol	$C_{20}H_{40}O$	296	16.251	15.01
2	Phytol acetate	$C_{22}H_{42}O_2$	338	16.251	15.01
3	Pentadecanal	$C_{15}H_{30}O$	226	16.251	15.01
4	Oxirane, 1,2-Epoxyoctadecane	$C_{18}H_{36}O$	268	16.251	15.01
6	Hexadecanal, Palmitaldehyde	$C_{16}H_{32}O$	240	16.251	15.01
8	Phytol	$C_{20}H_{40}O$	296	19.002	34.31
9	Cyclohexanol,5-methyl-2-(1-methylethyl),(1S,2R,5R)-(+),Menthol	$C_{10}H_{20}O$	156	19.002	34.31
14	13-Methyl-14-pentadecene-1,13-diol	$C_{16}H_{32}O_2$	256	19.002	34.31
15	Squalene	$C_{30}H_{5}0$	410	25.688	10.88
17	Eicosane	$C_{20}H_{42}$	282	30.752	17.88
19	2-methylhexacosane	$C_{27}H_{56}$	380	30.752	17.88
20	Tetratetracontane	$C_{44}H_{90}$	618	30.752	17.88
21	Hexatriacontane	$C_{36}H_{74}$	506	30.752	17.88
22	Pentadecane,8-n-Hexylpentadecane	$C_{21}H_{44}$	296	30.752	17.88

(B)

Peak no.	Compound	MF	MW (g/mol)	RT (min)	Area (%)
24	Hexanedioic acid, Adipic acid, Diisooctyl adipate, Bis(6-methylheptyl) hexanedioate	$C_{22}H_{42}O_4$	370	21.412	100
29	2-ethylhexyl pentadecyl ester	$C_{29}H_{56}O_4$	468	21.412	100
30	2-ethylhexyl tetradecyl ester	$C_{28}H_{54}O_4$	454	21.412	100

Key: MF = Molecular Formula; MW = Molecular Weight; RT = Retention time.

Table S2. Inhibitory action of Au-Ag BNPs and crude extracts on α-Amylase activity.

Samples	*In vitro* α-Amylase inhibition % at 2.0 mg/ml	p-value	IC_{50} (mg/ml) [a] 0.003-3.0 mg/ml [b] 0.002-2.0 mg/ml [c] 0.0002-2.0 mg/ml
Acarbose	48.27 ± 1.79	< .0001	0.022
BNPs (leaf)	69.97 ± 3.42 ***	< .0001	0.130 [c]
BNPs (flower)	60.57 ± 3.15 *	< .0001	0.196 [c]
Aq. dist. (flower)	58.03 ± 4.43	0.006	NT
Aq. dist. (leaf)	61.23 ± 5.24	0.007	0.029 [b]
60% EtOH (flower)	61.73 ± 6.37	0.011	NT
60% EtOH (leaf)	55.13 ± 9.17	0.027	0.033 [b]
70% EtOH (leaf)	55.81 ± 7.86	0.019	0.009 [a]

*Results are expressed as mean ± SEM; N = 3; p < 0.05, p-value summary * vs control; p-value < 0.0001, p-value summary *** vs control; NT = Not tested; Aq. dist. = Aqueous distillation.*